

## GLOBAL OCEAN CURRENT ENERGY ASSESSMENT: AN INITIAL LOOK

James H. VanZwieten<sup>a,b</sup>

Alana E. Smentek-Duerr<sup>b,c</sup>

Gabriel M. Alsenas<sup>b</sup>

Howard P. Hanson<sup>b</sup>

<sup>a</sup>Corresponding author: [jvanzwi@fau.edu](mailto:jvanzwi@fau.edu)

<sup>b</sup>Southeast National Marine Renewable Energy Center, Florida Atlantic University, Boca Raton, FL, USA

<sup>c</sup>Now at the U.S. Department of Energy, Wind Power Program, Washington, D.C., USA

### ABSTRACT

This paper provides an initial assessment of kinetic energy flux (power density per unit area) found in world-wide ocean current systems using results from a global ocean circulation model with comprehensive data assimilation. Three years (2009-2011) of Hybrid Coordinate Ocean Model-generated data were used to compare eight regions with time-averaged power density at least 500 W/m<sup>2</sup>. Included analysis and discussion is intended to provide a first look at potential ocean current energy harvesting locations around the world.

### INTRODUCTION

Energy in the world's oceans is found in either kinetic (i.e. waves, tides, or currents) or potential (i.e. thermal or salinity gradients) forms. Both types are presently being considered to generate useful electric power and various studies have discussed strategies for extracting marine renewable energy. Region-specific resource characterization studies have been performed for several U.S. locations and global resource characterization studies have been completed for ocean thermal energy [1,2,3] and wave energy [4]; however, comprehensive global ocean-current resource characterizations are not yet available. This study outlines model-based estimates of available ocean current energy globally and investigates some basic criteria helpful for preliminary commercial development-site identification.

Ocean-current energy is defined as the kinetic energy available in large-scale open-ocean geostrophic surface currents. These ocean currents generally exhibit strongest flow near the ocean's surface and have been studied over the past several decades as a potential source for generating electric power [5], especially in the Florida Current [5,6] and the Kuroshio Current [7]. More recently, several companies have proposed and designed ocean current turbines (OCTs) and some conceptual systems have already been tested in laboratories or under tow. Therefore, a study was needed to investigate and describe worldwide currents eligible for power generation.

Several parameters can be considered when investigating an OCT development site: an estimate of average available power (at various depths) helps to describe a flow's potential for power generation; variability of the flow's direction provides insights for mooring and turbine design; current speed extremes indicate survivability criteria and level of risk to equipment installed subsea; understanding the total water depth where currents are found helps to dictate potential mooring challenges; distances from the shore where currents are found provide information useful for transmission cabling and to compare capital costs for development in one current versus another; local cost of electricity can be evaluated to estimate economic drivers that might be favorable for one site over another, etc.

This study investigated several of the aforementioned parameters with Hybrid Coordinate Ocean Model (HYCOM)-predicted current data; the study did not, however, estimate overall power potential or consider local cost of electricity and grid interconnection. We first discuss HYCOM and its usefulness for this study. Next, we formulate and select time-averaged power densities in eight regions where the most significant ocean current resources are found worldwide. Then, a comparison of these regions with respect to one another includes discussion of various features. A summary follows.

## HYCOM

A 3-dimensional, real-time, ocean prediction simulator with a global  $1/12^\circ$  resolution [8] was used for this study. The Hybrid Coordinate Ocean Model (HYCOM) incorporates data assimilation to produce, via a 5-day hindcast/forecast scheme, global datasets with daily snapshots of eastward and northward velocities, salinity, sea-surface height, and ocean temperature. The HYCOM model version used by this study assimilates observed data from both historical and near real-time measurements by satellites and *in situ* instruments (ocean currents, sea-surface temperature and sea-surface height), CTDs and moorings (temperature and salinity profiles), and the Special Sensor Microwave Imager [9].

The vertical coordinate scheme utilized by HYCOM is one of its notable features [8]. Typically, ocean models employ discrete intervals of depth, discrete intervals of density, or follow ocean bottom terrain for the vertical coordinate structure. However, these schemes are not best suited to all portions of the ocean. An isopycnal structure is efficient for deep ocean modeling, constant depth or pressure schemes are best for mixed layer modeling, a terrain-following coordinate approach is best suited for coastal regions, and very shallow regions work well with level coordinates. HYCOM combines all four vertical coordinate schemes, in regions where they are best suited, with a smooth transition between each region.

Originally developed as an oceanographic research tool, HYCOM has been considerably validated with observations, and its use as an operational forecasting model demonstrates both

its versatility and its verisimilitude. Biases and inaccuracies in the model are continually being discovered and corrected. HYCOM's usefulness for MRE power estimates was discussed at length recently [6], and given the relative paucity of oceanic observations on a global scale, model results of this nature represent a useful first step in providing guidance toward regions ripe for MRE development.

Specifically, this study selected once-daily HYCOM data sets for the period 1 January 2009 – 31 December 2011. These dates were chosen to ensure water velocity estimates were derived from the most recent HYCOM versions (versions 90.6, 90.8 and 90.9) and to benefit from other update improvements. Complete consecutive years were chosen to allow for seasonal variations. HYCOM datasets, including the ones used for this study, are publicly available through the community web site at <http://www.hycom.org>.

## POWER DENSITY

To help identify regions that could potentially be desirable for commercial utility-scale ocean current electricity generation, power density (i.e., the kinetic energy flux) is a useful metric. While power density does not independently imply the total energy that can be extracted from an ocean current, it does provide significant insight into the energy that can be extracted by either a single OCT or a small array of turbines. The power density available to a turbine (unit area perpendicular to a flow) is calculated from

$$P = \frac{1}{2}\rho V^3, \quad (1)$$

where  $P$  is kinetic energy flux or power density per unit area,  $\rho$  is the density of seawater, and  $V$  is free-stream current magnitude. To evaluate a more practical amount of extractable power for a particular turbine technology (or small array where OCTs extract only a fraction of the energy in the flow), the product of a power coefficient and kinetic energy flux is an estimate of the extractable power per unit area swept by a turbine exposed to a flow, or

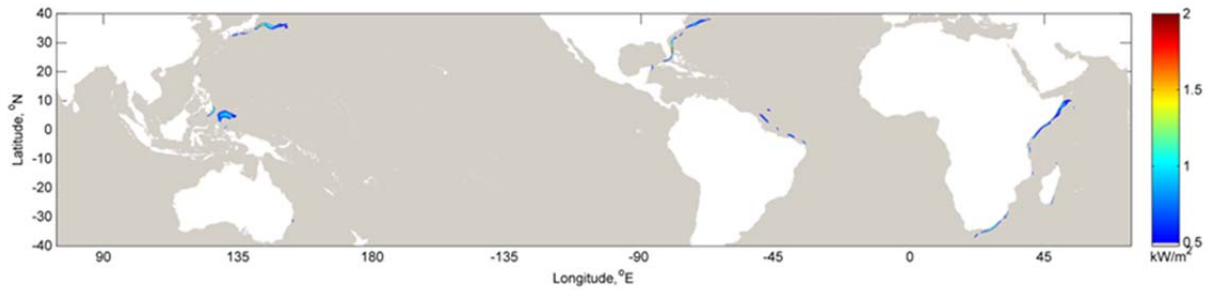


**FIGURE 1: THREE YEAR (2009-2011) HYCOM-CALCULATED AREAS WITH TIME-AVERAGED POWER DENSITIES GREATER THAN 0.5KW/M<sup>3</sup> AT 50 M DEPTH.**

$$P_e = C_{P_e} P. \quad (2)$$

Here,  $P_e$  is the extractable power output per unit area and  $C_{P_e}$  accounts for hydrodynamic efficiencies, electromechanical efficiencies, and power transmission/conversion efficiencies. This value is turbine- and location-specific, and is dependent on flow speed, design, and other operating characteristics. For example, hydrodynamic efficiencies for vertical-axis turbines typically exhibit maxima of around 0.35 (e.g., [10]), while horizontal-axis rotors typically exhibit maxima of around 0.45 [11,12].

When exposed to flow speeds slower than its cut-in speed (the current speed at which the rotor begins to generate lift and overcome drive train friction), an OCT will not be capable of generating electricity from the flow. Conversely, at extremely high current speeds, an OCT will be forced to brake or “shed” power to avoid system failures,

further limiting the amount of power practically achievable from a flow. Therefore, it is generally accepted that OCTs will convert somewhere between 25% and 40% of the available power density per unit area (the swept area of the rotor in this case) into grid-useful electricity.

While this study primarily evaluates power density ( $P$ ) for various regions, the use of extractable power output ( $P_e$ ) is reserved for discussion examples. Assumed or estimated  $C_{P_e}$  values are indicated when used.

### Study Region Selection

To estimate average power that a single turbine (or array of OCTs) might possibly extract at various locations worldwide, power density ( $P$ ) was calculated for each global HYCOM grid point at depths of 0, 30, 50, 75, 100, and 150 m. Daily  $P$  was then averaged over a three year period at each grid point ( $\bar{P}$ ). To focus the study, areas that

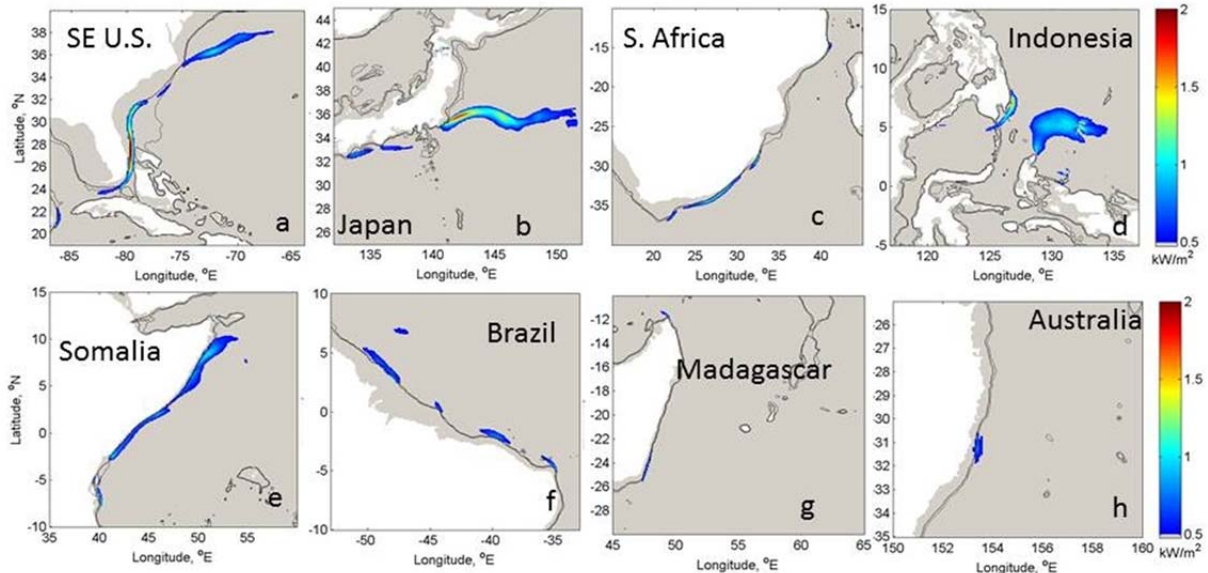


**FIGURE 2: EIGHT REGIONS WITH CONCENTRATED TIME-AVERAGED KINETIC ENERGY FLUX IN EXCESS OF 0.5 KW/M<sup>2</sup> BETWEEN 2009 AND 2011 AT A DEPTH OF 50 M. 500 M (BLACK) AND 1000 M (DARK GREY) CONTOUR LINES ARE INCLUDED FOR REFERENCE.**

might be minimally eligible for consideration as OCT production sites were assigned a minimum average power density of 0.5 kW/m<sup>2</sup>. Areas with power densities less than this amount might not be economically desirable locations for utility-scale generation, and were therefore excluded from this analysis. As well, this choice ensures consistency with a “hot spot” definition utilized by a recently published tidal energy resource assessment [13].

To assemble candidate global grid points into regions (currents), an initial evaluation depth of 50 m was selected as a reasonable shallowest “hub height” for OCTs. Because it is considered ideal to operate large turbines below vessel traffic and to avoid undesirable forcing from ordinary surface waves, this choice was suitable for an initial review. As well, OCTs at this depth could still be installed within adequate proximity to the sea surface, where ocean current flows are typically stronger.

Using this methodology, grid points were grouped into eight regions which are presented graphically in Figure 2. In all resource maps, land and freshwater areas are shaded white, while areas with less than 0.5 kW/m<sup>2</sup> mean power density are shaded grey. Using these groupings, it was then possible to evaluate depths where average power density was greatest for each region. In Figure 3, a spatial average of  $\bar{P}$  in each of the eight evaluated current regions is presented as a function of depth. This analysis indicates that average power density significantly *decreases* with depth in all regions. This effect is most apparent in the North Agulhas current where the average power density at a depth of 100 meters is only

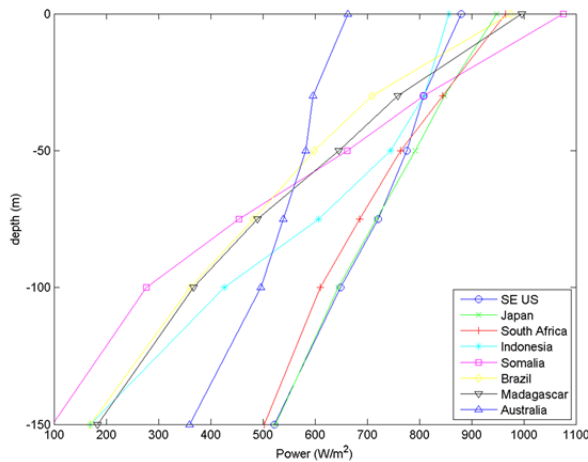


**FIGURE 3: HYCOM TIME-AVERAGED KINETIC ENERGY DENSITY FLUX, AVERAGED ACROSS EACH CURRENT REGION AND PRESENTED AS A FUNCTION OF DEPTH.**

26% of available average power density at the surface. However, in certain regions like the East Australia and Gulf Stream currents, average power density is relatively consistent over a greater depth, and average available power density at 100 m is 75% and 74% of the available energy density at the sea surface, respectively. Globally, however, at all evaluated grid points with time-averaged power density greater than 0.5 kW/m<sup>2</sup>, only 53% of this power density is found at 100 m while 78% is located at 50 m.

The study therefore concluded that all regions exhibit greatest total available average power density at approximately 50 m of depth (when assuming OCTs must be submerged fully, below ship traffic), which provided sufficient confidence that our earlier depth estimate did, in fact, include the most energetic grid points, and consequently, would represent what appears to be the most desirable depth for commercial investigation, and this study. Therefore, subsequent power calculations presented in this analysis are exclusively selected from 50 m depths.

### Power Density in Regions

Spatial averages ( $\bar{P}_{Avg}$ ), normalized standard deviations ( $\sigma_p/\bar{P}$ ) and maximum ( $\bar{P}_{Max}$ ) power densities in each region were calculated (Table 1) to provide a preliminary basis for comparison of regions. The  $\bar{P}_{Avg}$  value represents a spatial average of all previously time-averaged grid points greater than 0.5 kW/m<sup>2</sup>. Although the maximum time-averaged power density in any region was 1.93kW/m<sup>2</sup> (offshore the east coast of Florida, USA), three others exhibited  $\bar{P}_{Max}$  values within 20% (Japan, South Africa, and Indonesia regions).

Table 1 also provides calculated areas of the sea surface (in km<sup>2</sup>) where time-averaged power densities greater than 0.5, 1.0 and 1.5 kW/m<sup>2</sup> were identified. At a depth of 50 meters, nearly 836,000 km<sup>2</sup> of the world’s sea surface exhibits an available time-averaged power density greater than 0.5kW/m<sup>2</sup> (approximately the combined size of U.S. states Texas and Arkansas). Of that area, though, only 10% is more energy dense than 1.0 kW/m<sup>2</sup>, and 2% greater than 1.5 kW/m<sup>2</sup>. This, of course, suggests that OCTs designed with greater efficiency at slower flow speeds will be compatible with more regions.

**TABLE 2: AREAS OF THE SEA SURFACE, BY CURRENT REGION, CALCULATED FROM THREE YEAR AVERAGED (2009-2011) HYCOM DATA, AT A DEPTH OF 50 M, REPRESENTING GREATER THAN 0.5, 1.0, 1.5 kW/M<sup>2</sup> TIME-AVERAGED POWER DENSITIES.**

<b>Region</b>	<b>Associated Current</b>	$\bar{P}_{Avg}$ (kW/m <sup>2</sup> )	$\sigma_P/\bar{P}$	$\bar{P}_{Max}$ (kW/m <sup>2</sup> )	$A_{0.5}$ (km <sup>2</sup> )	$A_{1.0}$ (km <sup>2</sup> )	$A_{1.5}$ (km <sup>2</sup> )
<b>Southeast US (Fig. 2a)</b>	Gulf Stream	0.776	0.949	1.93	144,830	25,871	7,537
<b>Japan (Fig. 2b)</b>	Kuroshio	0.792	1.34	1.78	173,401	37,309	5,840
<b>South Africa (Fig. 2c)</b>	Agulhas (South)	0.764	1.09	1.66	68,055	12,987	225
<b>Indonesia (Fig. 2d)</b>	Equatorial Currents	0.744	2.18	1.57	196,518	8,696	681
<b>Somalia (Fig. 2e)</b>	Agulhas (North)	0.661	1.79	1.34	182,827	2,425	0
<b>Brazil (Fig. 2f)</b>	North Brazil Current	0.598	1.15	1.08	57,338	169	0
<b>Madagascar (Fig. 2g)</b>	Mozambique	0.645	0.979	0.86	8,570	0	0
<b>Australia (Fig. 2h)</b>	Eastern Australian	0.582	1.20	0.73	4,365	0	0
<b>Total</b>	-	<b>0.696<sup>1</sup></b>	<b>1.34<sup>1</sup></b>	<b>1.369<sup>1</sup></b>	<b>835,904</b>	<b>87,457</b>	<b>14,283</b>

<sup>1</sup> Mean of values above

While most current regions offer some sea surface area with energy densities greater than 1.0 kW/m<sup>2</sup> (with the exception of Madagascar and Australia current regions), the Southeast U.S. and Japan regions boast areas with average power density greater than 1.5 kW/m<sup>2</sup> that are a full order of magnitude larger than the rest. Interestingly, when considering all areas of the sea surface with average power densities greater than 1.5 kW/m<sup>2</sup> worldwide, the Southeast U.S. region occupies more surface area than all other areas combined.

For illustration purposes, at a 1.5 kW/m<sup>2</sup> power density ( $\bar{P}$ ), assuming an average overall efficiency ( $C_{pe}$ ) of 35% and ignoring contributions from vertical current shear, a single turbine with a 30 m diameter rotor (swept area of 707 m<sup>2</sup>), installed at a 50 m depth, could, for example, produce about 3.25 GW-h annually (Equation 2 multiplied by swept area and the number of hours per year). Based upon a U.S. Energy Information Administration estimate that an average U.S. home consumed 11,280 kWh in 2011 [14], this hypothetical turbine could power approximately 288 homes. It is also interesting to compare ocean current average power densities with more mature renewables. Assuming average atmospheric conditions ( $\rho=1.2$  kg/m<sup>3</sup>), a 10 m/s

wind would yield approximately 0.6 kW/m<sup>2</sup> of kinetic energy density. Likewise, assuming average solar insolation (without atmospheric influence), a square meter of earth could be exposed to 0.342 kW/m<sup>2</sup> of solar radiation over the course of a day. Based upon our results, ocean currents could provide 0.696 kW/m<sup>2</sup> (Table 1) on average.

Ultimately, translating power densities into practical energy recovery depends on a variety of assumptions and is beyond the scope of this study. However, these results suggest that continued interest in these current systems as a source of renewable energy appears worthwhile.

#### Variability of Power Density

How much the time-averaged power density varies in the regions identified with at least 0.5 kW/m<sup>2</sup> is also useful to investigate. By calculating the standard deviation ( $\sigma_P$ ) of power density ( $P$ ) at each HYCOM grid point over time, we determine a deviation value at each point, and each region can then be evaluated. To make these values more meaningful, they were normalized over the time-averaged power density ( $\bar{P}$ ) at each grid point, resulting in a fractional representation,  $\sigma_P/\bar{P}$ .

This  $\sigma_P/\bar{P}$  value was spatially-averaged across each region to determine a representative normalized variability (Table 1). Each region's normalized variability is also represented spatially in Figure 4. Although the spatially-averaged region values in Table 1 appear to be high, many regions exhibit substantial areas with lower variability. In the Southeast U.S. region, for example, in the Florida Straits Gulf Stream "core" area which represents the region's highest average flow speeds, the minimum normalized variability is 0.35. This is similarly true in the Japan region, where the minimum normalized variability in the Tsugaru Straits is 0.34; although this area is not flow associated with the primary Kuroshio Current, it may be of local development interest. Other notable minimum normalized variability regions include Somalia (0.60), Brazil (0.64), and South Africa (0.83).

The  $\sigma_P/\bar{P}$  normalized variability was also investigated for the most energy dense areas of global current regions, those above 1.5 kW/m<sup>2</sup>. Globally, the average of all areas is 0.68, significantly less than the normalized variability of regions with at least 0.5 kW/m<sup>2</sup> (1.34). More specifically, the Southeast U.S. region is the least variable (0.44), while the other three regions in ascending order are: Indonesia (0.84), Japan (0.94) and South Africa (1.12). The normalized variability of power density in high current areas is typically significantly less than areas with lower average power densities. Areas with less than 50% variability are present globally, and with careful site selection, both average power density

and acceptable consistency can be identified.

### Location of Power Density

Where useful power densities can be found is a feature also evaluated by this study. The distance between each grid point that met minimum  $\bar{P}$  criteria (0.5 kW/m<sup>2</sup> at 50 m) and the closest "dry" point was calculated. Although this automatic methodology did not ensure a populated land area was selected, the results provide a basic insight into proximities between land areas (potential transmission interconnection locations) and offshore ocean current resources.

Figure 5a indicates each region's area, as a function of distance, to the closest land mass. Figure 5b includes only sea surface areas which were located within 25 km of land. Of all eight regions, Japan is the closest proximity to shore (some grid points are within 7 km). Grid points offshore South Africa (11 km), Southeast US (11.5 km), Somalia (12 km), and Indonesia (12.2 km) were all identified within 15 km of land. Closer inspection of the three closest regions, however, indicates wide diversity in distribution with respect to one another. Japan's current is located primarily between 75 and 100 km from a shoreline (64%), while South Africa's current is evenly distributed between 25 and 100 km (27% between 25 and 50 km, 22% between 50 and 75 km, 21% between 75 and 100 km, and 21% greater than 100 km), and in the Southeast U.S., about a third is found within 100 km (33%).

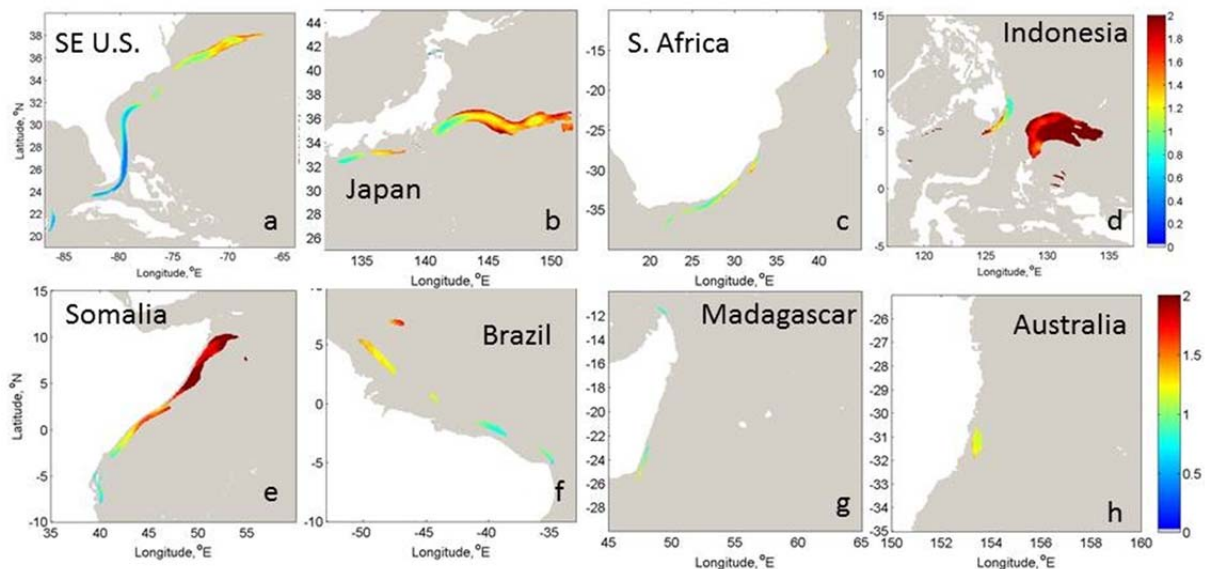
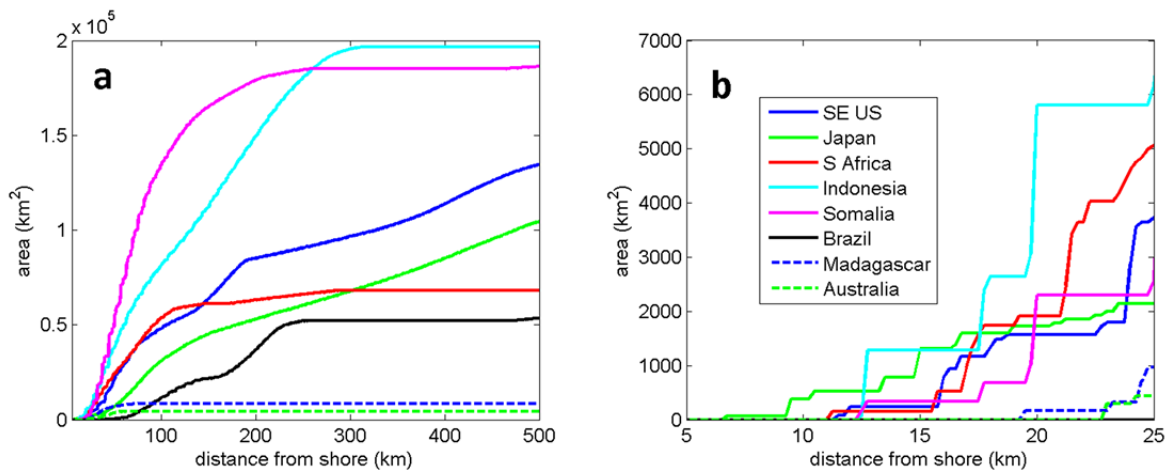


FIGURE 4: NORMALIZED STANDARD DEVIATION OF POWER DENSITY (AT LEAST 0.5 KW/M<sup>2</sup>), AT A DEPTH OF 50 METERS, IN EACH OF THE EIGHT MAJOR GLOBAL CURRENT REGIONS IDENTIFIED.



**FIGURE 5: SEA SURFACE AREA WITH TIME-AVERAGED POWER DENSITY OF AT LEAST 0.5 kW/M<sup>2</sup>, AT A DEPTH OF 50 METERS, WITH RESPECT TO CLOSEST LAND. SUBFIGURE B INDICATES ONLY AREAS WITHIN 25 KM OF LAND.**

Globally, of all  $\bar{P}$  greater than 0.5 kW/m<sup>2</sup>, slightly more than 2% ( $1.67 \times 10^4$  km<sup>2</sup>) is within 25 km of land, 18% ( $1.50 \times 10^5$  km<sup>2</sup>) within 50 km, 33% ( $3.68 \times 10^5$  km<sup>2</sup>) within 75 km, and 44% within 100 km. However, globally across regions with significant average power density (grid points with  $\bar{P}$  greater than 1.5 kW/m<sup>2</sup>), much greater proportions were located closer to shore (75%,  $1.07 \times 10^4$  km<sup>2</sup>, within 100 km).

Another location feature this study explored with HYCOM data was overall water depth below energy-dense ocean current areas. How shallow or deep areas correspond to available power density offshore indicates the technical challenges that may be present for anchoring or mooring OCTs. Figures 2a-h include isobaths which correspond to depths of 500 and 1,000 m to help visualize bottom depths near current regions. Table 2 also summarizes percentages of areas, globally, which correspond to various bottom depths for  $\bar{P}$  values corresponding to 0.5 and 1.5 kW/m<sup>2</sup>.

Although the vast majority of sea surface area with at least 0.5 kW/m<sup>2</sup> was identified in water depths greater than 2,000 m (67%), more concentrated average power densities (greater than 1.5 kW/m<sup>2</sup>) are found shallower, between 400 and 800 m (54%). Figures 6a and 6b present sea surface areas with at least 0.5 kW/m<sup>2</sup> average power density as a function of ocean bottom depth in each region. These minimum  $\bar{P}$  values are found in water depths less than 100 m in Japan and Somalia; 125 m in the Brazil region; 150 m depths off Madagascar and the Southeast U.S., and 200 m depths in South Africa, Indonesia, and Australia. However, these depths correspond to small areas and are not representative of regional characteristics.

In the Southeast U.S. region, most of the average power density is located in water depths greater than 300 m, with 3% located in water depths less than 400 m, 68% located in water depths less than 600 m, and no  $\bar{P}$  values were located in water depths greater than 800 m. The Japan region's resource is located in deep water depths, with 1% less than 200 m, 2% located in water depths less than 400 m, and only up to 10% was found in water depths less than 1,000 m. South Africa's current resource is entirely located in water depths between 600 and 1,000 m (67% less than 800 m and 100% less than 1,000 m).

Bottom depths corresponding to high average power density (greater than 1.5 kW/m<sup>2</sup>) in the Southeast U.S. region were similar to the global distribution of minimum average power density, where 65% is found in bottom depths between

**TABLE 2: AREAS OF THE SEA SURFACE WITH TIME-AVERAGED POWER DENSITIES GREATER THAN 0.5 AND 1.5 kW/M<sup>2</sup> AS A FUNCTION OF BOTTOM DEPTH.**

Bottom Depth (m)	$A_{0.5}$ (%)	$A_{1.5}$ (%)
< 200	0.5	0.5
200-400	2.7	2.1
400-600	4.8	35
600-800	6.1	19
800-1,000	4.0	1.5
1,000-2,000	15	6.8
> 2,000	67	35

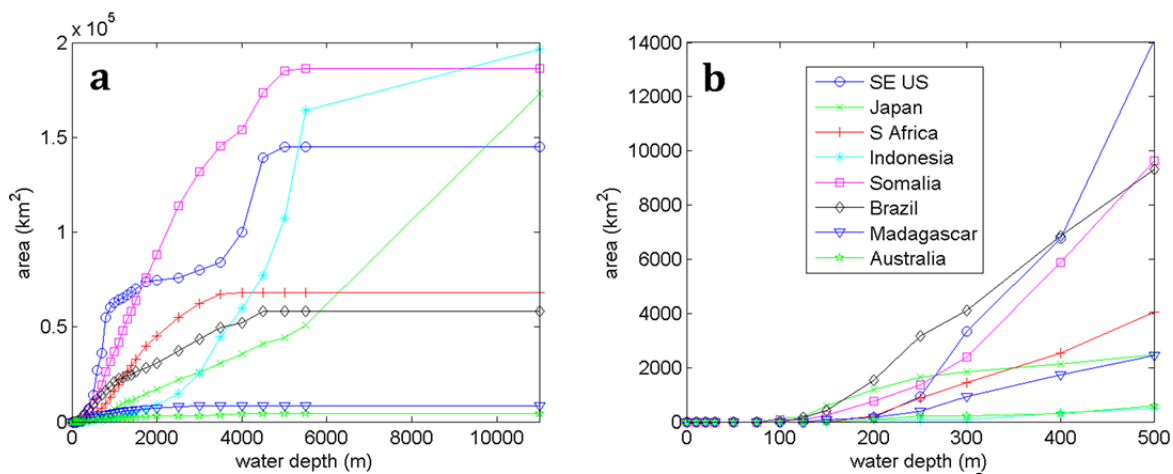


**FIGURE 6: SEA SURFACE AREA WITH TIME-AVERAGED POWER DENSITY OF AT LEAST 0.5 kW/M<sup>2</sup>, AT A DEPTH OF 50 METERS, AS A FUNCTION OF OCEAN BOTTOM DEPTH. SUBFIGURE B INDICATES ONLY AREAS SHALLOWER THAN 500 M DEPTH.**

400 and 600 m and 32% between 600 and 800 m. This appears to be similarly true for the South Africa region, but slightly deeper, where 67% is found between 600 and 800 m and 33% between 800 and 1,000 m. In the Japan region, average power densities greater than 1.5 kW/m<sup>2</sup> are found in deep water, with more than 73% found in water deeper than 2,000 m, 17% is between 1,000 and 2,000 m depth, and the rest is fairly distributed, (less than 3% is shallower than 400 m and 7% is found between 400 and 1,000 m).

## CONCLUSION

Open-ocean currents such as the Gulf Stream, Agulhas, and Kuroshio occur in all the world's ocean basins, and MHK energy resources are associated with many of them. The richest of these resources, off the Southeast coast of the U.S., is by no means the only one that offers a potential for significant energy recovery.

This study evaluated global ocean current energy resources with three years of HYCOM-predicted simulation data. Time-averaged kinetic energy (power) densities were calculated at each grid point at a 50 m depth, and points which exceeded 0.5 kW/m<sup>2</sup> were used to define eight regions of interest. Those regions were compared by various traits, including max average power density, distances from land, areas of sea surface with selected average power densities, depth of sea floor, and standard deviation.

Ultimately, the degree to which commercial-scale deployments of ocean-energy recovery systems succeeds will depend on a variety of factors in addition to the characteristics of the resource at a particular location. This study

provides only a first look at the power densities associated with the resources in various locations and does not address these other factors. The authors expect to conduct further studies to leverage HYCOM as a useful ocean current resource evaluation tool.

*Acknowledgements:* The SNMREC is supported by the State of Florida and by the U.S. Department of Energy. The views expressed here are solely those of the authors.

## REFERENCES

- [1] Nihous, G.C., 2010, "Mapping Available Ocean Thermal Energy Conversion Resources Around the Main Hawaiian Islands with State-of-the-Art Tools," J. Renewable Sustainable Energy, Vol. 2, 043104-1-9.
- [2] Rauchenstein, L.T., 2012, "Global Distribution of Ocean Thermal Energy Conversion (OTEC) Resources and Applicability in U.S. Waters Near Florida," MS Thesis. Florida Atlantic University, Boca Raton, FL, 2012.
- [3] Ascari, M., H. P. Hanson, L. Rauchenstein, J. VanZwieten, D. Bharathan, D. Heimiller, N. Langle, G.N. Scott, J. Potemra, E. Jansen, John Nagurny, 2012, "Ocean Thermal Extractable Energy Visualization: Final Report," U.S. Department of Energy, Washington, DC.
- [4] Cornett, A. M., 2008, "A Global Wave Energy Resource Assessment," Proceedings of the International Offshore and Polar Engineering Conference, Vancouver, Canada, July 6 - 11, no. ISOPE-2008-579.
- [5] Von Arx, W.S., H.B. Stewart, and J.R. Apel, 1974, "The Florida Current as a Potential Source of Useable



- 
- Energy,” Proceedings of the MacArthur Workshop on the Feasibility of Extracting Usable energy from the Florida Current, Palm Beach Shores, Florida.
- [6] Duerr, A.E.S., M.R. Dhanak, and J. Van Zwieten, 2012, “Utilizing the Hybrid Coordinate Ocean Model Data for the Assessment of the Florida Current’s Hydrokinetic Renewable Energy Resource,” Marine Technology Society Journal, vol. 12, pp. 24-33.
- [7] Chen, F., 2010, Kuroshio Power Plant Sevelopment Plan. Journal of Renewable and Sustainable Energy Reviews, Vol. 14, pp 2655-2668.
- [8] Chassignet, E.P, H.E. Hurlburt, E.J. Metzger, O.M. Smedstad, J.A. Cummings, G.R. Halliwell, R. Bleck, R. Baraille, A.J. Wallcraft, C. Lozano, H.L. Tolman, A. Srinivasan, S. Hankin, P. Cornillon, R. Weisberg, A. Barth, R. He, F. Werner, and J. Wilkin, 2009, “US GODAE Global Ocean Prediction with the HYbrid Coordinate Ocean Model (HYCOM),” Oceanography, NOPP Special Issue, Vol. 22, pp. 64-75.
- [9] Chassignet, E.P, H.E. Hurlburt, O.M. Smedstad, G.R. Halliwell, P.J. Hogan, A.J. Wallcraft, R. Baraille, and R. Bleck, 2007, “The HYCOM (HYbrid Coordinate Ocean Model) Data Assimilative System,” Journal of Marine Systems, 65, 60-83.
- [10] Hau, E., 2006, “Wind Turbines: Fundamentals, Technologies, Application, Economics,” Springer-Verlag, Berlin, 624 pp. ISBN 3-540-57064-0.
- [11] Bahaj, A. S., A.F. Molland, J.R. Chaplin, and W.M.J. Batten, 2007, “Power and Thrust Measurements of Marine Current Turbines Under Hydrodynamic Flow Conditions in a Cavitation Tunnel and a Towing Tank”, Journal of Renewable Energy, vol. 32, pp. 407-426.
- [12] Van Zwieten, J. H., Jr., C.M. Oster, and A.E.S. Duerr. 2011, “Design and Analysis of a Rotor Blade Optimized for Extracting Energy from the Florida Current,” Proceedings of the ASME 2011 International Conference on Ocean, Offshore, and Arctic Engineering, Rotterdam, Netherlands, June 19-24, no. OMAE2011-49140.
- [13] Georgia Tech Research Corp., 2011, “Assessment of Energy Production Potential from Tidal Streams in the United States,” Final Project Report, U.S. Department of Energy, Washington, D.C. Available at: <http://www1.eere.energy.gov/water/pdfs/1023527.pdf>.
- [14] U.S. Department of Energy, 2013, “FREQUENTLY ASKED QUESTIONS: How much electricity does an American home use?”, Energy and Information Administration, Washington, D.C., Available at: <http://www.eia.gov/tools/faqs/faq.cfm?id=97&t=3>.